Electronic Supplementary Material (ESI) for Physical Chemistry Chemical Physics.

A comparative study on modeling of ferromagnetic and paramagnetic states of uranium hydride using DFT+U method

Supplementary Information

KyuJung Jun[1, 2, 3], Jae-Uk Lee[4], Min Ho Chang[4], Takuji Oda[1, *]

[1] Department of Nuclear Engineering, Seoul National University, 1 Gwanak-ro, Gwanak-gu, Seoul 08826, Republic of Korea

[2] Department of Materials Science and Engineering, University of California Berkeley, Berkeley, California 94720, United States

[3] Materials Science Division, Lawrence Berkeley National Laboratory, Berkeley, California 94720, United States

[4] National Fusion Research Institute, 52 Eoeun-dong, Yuseong-gu, Daejeon 34133, Republic of Korea

*Corresponding Author: oda@snu.ac.kr, +82-8-880-8988

Supplementary Figure S1. Structural information and polyhedral connectivity of both $\alpha - UH_3$ and $\beta - UH_3$. Figures (a) and (b) show the unit-cells of both phases from the (100) plane of the cubic lattice. Figures (c) and (d) show the polyhedral connectivity of both phases. 12-fold coordination of hydrogen around a uranium atom can be found. The green spheres represent linear-chain U atoms (U^1). The blue spheres represent U atoms on BCC sublattice (U^2).

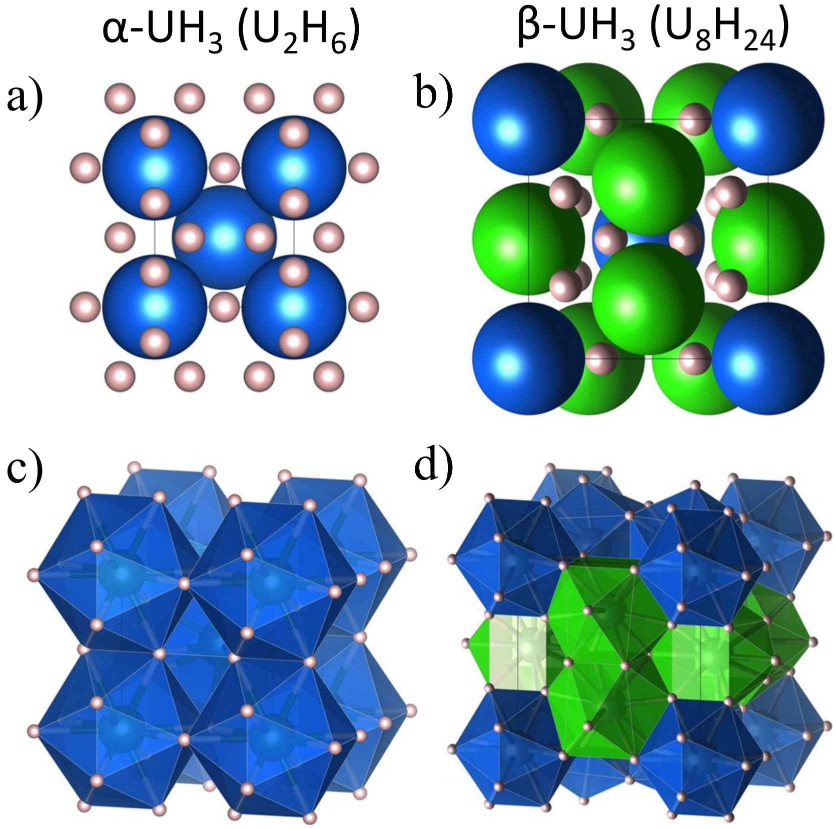

Supplementary Table S1. ZPE corrected formation energies and lattice constants of both phases with respect to various calculation conditions. The ZPE correction for all conditions was made using the correction value calculated with PBE functional as explained in Section 3.1 of the main body. For the name of calculation condition, following the functional type, SO stands for spin-orbit coupling, SP stands for spin-polarized calculation, and the number after 'U' (such as 0.2 for PBE-SP-U0.2) stands for the U_{eff} value that was used.

Calculation Condition	ZPE Corrected Formation Energy (eV)		Lattice Constant (Å)	
	α-UH_3	β-UH_3	α-UH_3	β-UH_3
PBE-SO	-0.981	-1.018	4.125	6.592
PBE-SP-U0.0	-0.930	-0.949	4.120	6.587
PBE-SP-U0.2	-1.016	-1.036	4.124	6.598
PBE-SP-U0.4	-1.102	-1.126	4.129	6.608
PBE-SP-U0.6	-1.190	-1.221	4.134	6.619
PBE-SP-U0.8	-1.279	-1.319	4.139	6.630
PBE-SP-U1.0	-1.368	-1.423	4.144	6.643
LDA-SO	-1.245	-1.258	4.007	6.431
LDA-SP-U0.0	-1.173	-1.181	3.993	6.397
LDA-SP-U1.0	-1.548	-1.555	4.053	6.482
LDA-SP-U2.0	-2.003	-2.086	4.080	6.547
RTPSS	-1.030	-1.019	4.112	6.572
SCAN	-0.734	-0.930	4.095	6.628

Supplementary Figure S2. Radial distribution function of two phases of uranium hydride.

The quality of an SQS structure is determined by how well it matches the correlations of the fully disordered state. In practice, short-range correlations are preferably matched compared to long-range interactions because distant neighbors hardly contribute to the spin interaction. In order to determine the cutoff distance of interactions, radial distribution function (RDF) is generated in Figure S2. The black lines represent two of the cutoff radii that we tested for the pair correlations, namely, 8 Å and 10 Å. Even the fourth neighboring uranium atoms are well within the 8 Å cutoff.

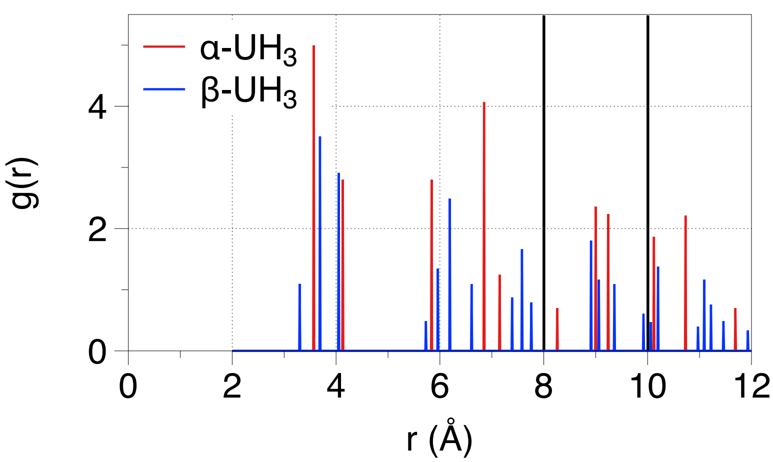

Supplementary Figure S3. Generation of SQS structure and error of correlation in the SQS structure used in the present study.

The error of correlation of pair and triplet interactions that we compared for both phases are drawn in Figure S3. Since the concentration of up-spin and down-spin uranium atoms are both 0.5, the correlation value of perfectly random structure is exactly zero. In case of $\alpha - UH_3$, both cutoff radii sets, (10 Å, 8 Å) and (8 Å, 6 Å) for (Pair, Triplet), show near perfectly random distribution. $\beta - UH_3$ show some improvement when using (10 Å, 8 Å) as perfectly random distribution is achieved up to larger distance compared to the case of (8 Å, 6 Å). The correlations start to show deviation from perfectly random distribution at approximately 6 Å. However, based on cluster expansion formalism[1], what determines the materials properties the most is not the overall error of all interactions, but only the nearby interactions up to a certain distance. In our structures, the correlations up to 6.1 Å match that of a perfectly random distribution with (10 Å, 8 Å). In a previous study for magnetic Fe-Cr alloy[2], it was shown that an SQS generated using (6 Å, 5.2 Å) results in a set of exactly reproduced correlations up to 1.5 times the distance to the nearest neighbor. The nearest neighbor radius for this material was approximately 3.32-3.61 Å, which is comparable to those in both phases of uranium hydride. Therefore, we consider that the two settings, namely, (10 Å, 8 Å) and (8 Å, 6 Å), can safely account for sufficiently distant interactions.

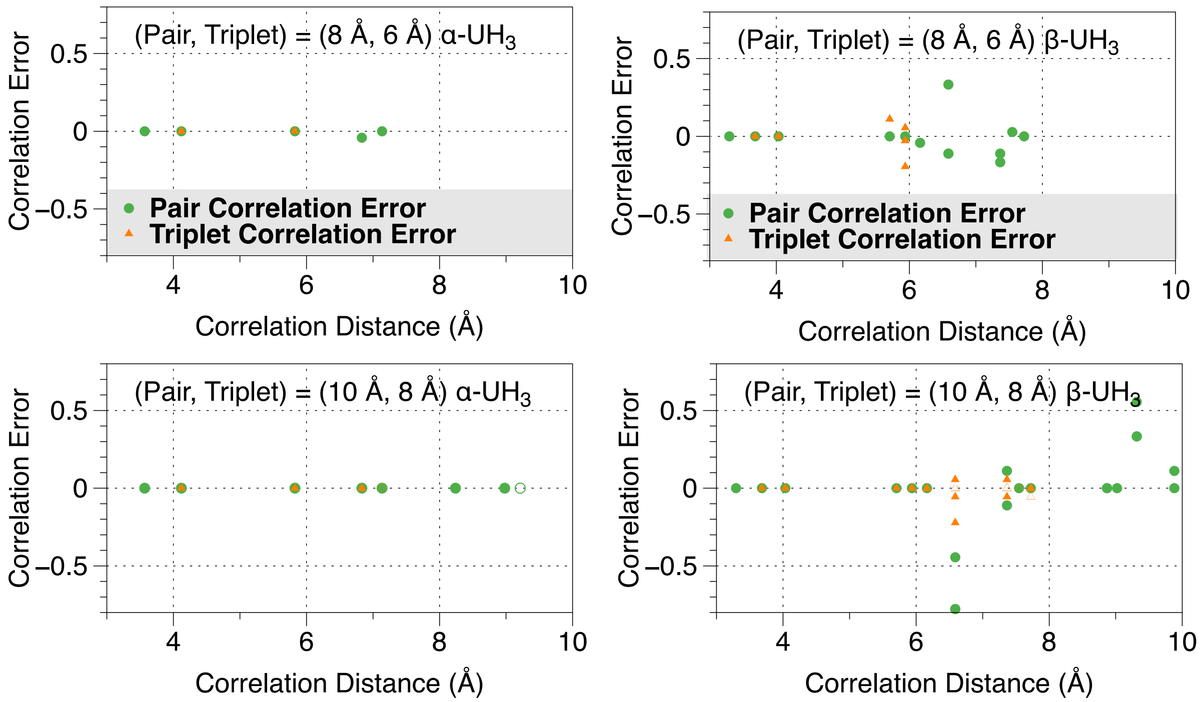

In theory, by using a supercell of infinite size, we can always achieve a perfectly disordered distribution of clusters. However, not only is this difficult to achieve due to the high computational cost of large-scale simulations, this is not always necessary because materials properties tend to be affected the most by the nearest neighbors and quickly converge within a small distance. Figure 2 of the main body corroborates this point by showing that the formation energy of the two correlation sets already converge at supercell size of SQS32. In addition, for both phases, the lattice constants converge below 0.1 Å per unit cell at the supercell size of SQS32. The small difference between the result of the two correlation sets indicate that our choice of distances is sufficient enough to capture the materials properties accurately. In conclusion, these two sets of correlation distances are the range where we can achieve sufficient accuracy and at the same time, the supercell does not become excessively large. Since it is always more accurate to include longer distance interactions, we safely chose the set (Pair, Triplet) = (10 Å, 8 Å).

Supplementary Figure S4. Phonon dispersion curves of (a) Pm-3n and (b) R3C structure of $\beta - UH_3$ using PBE+U(0.6) functional.

Phonon dispersion curves of Pm-3n $\beta - UH_3$ obtained with PBE+U(0.6) are provided in Figure (a). There exist three phonon modes having imaginary frequencies at the gamma point (symmetric x, y, z direction). By displacing the atoms toward the eigenvectors of these modes, an R3C structure was obtained. As seen in Figure (b), there are no modes having imaginary frequencies in the R3C structure. In addition, an interactive visualization[4] is provided via the link below. Each of the vibration modes is shown with the corresponding motion of atoms, not only for the imaginary phonons, but all phonon modes.

Pm-3n

http://henriquemiranda.github.io/phononwebsite/phonon.html?yaml=https://raw.githubusercontent.com/KyuJungJun/UraniumHydride-Imaginary-Phonon-Frequency/master/b-UH3-phonon-dispersion/band_pm-3n.yaml&name=b-UH3-Pm-3n

R3C

http://henriquemiranda.github.io/phononwebsite/phonon.html?yaml=https://raw.githubusercontent.com/KyuJungJun/UraniumHydride-Imaginary-Phonon-Frequency/master/b-UH3-phonon-dispersion/band_r3c.yaml&name=b-UH3-R3C

a) Pm-3n

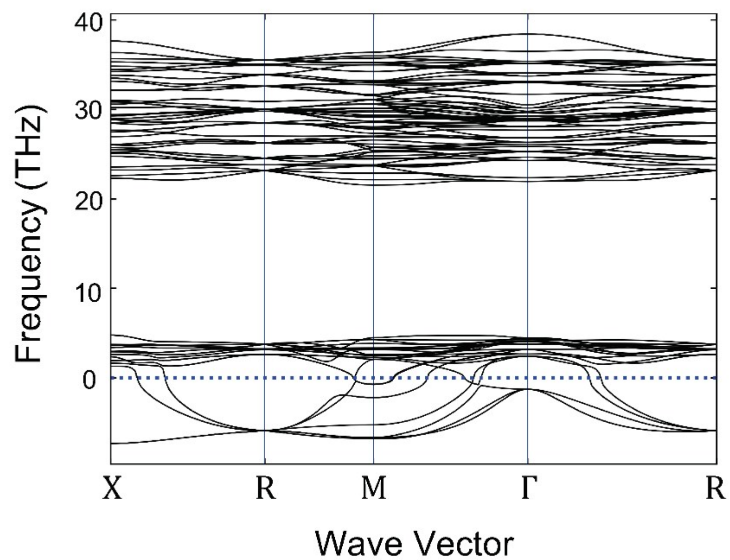
40
30
20
10
0
Frequency (THz)
X
R
M
Γ
R
Wave Vector

b) R3C

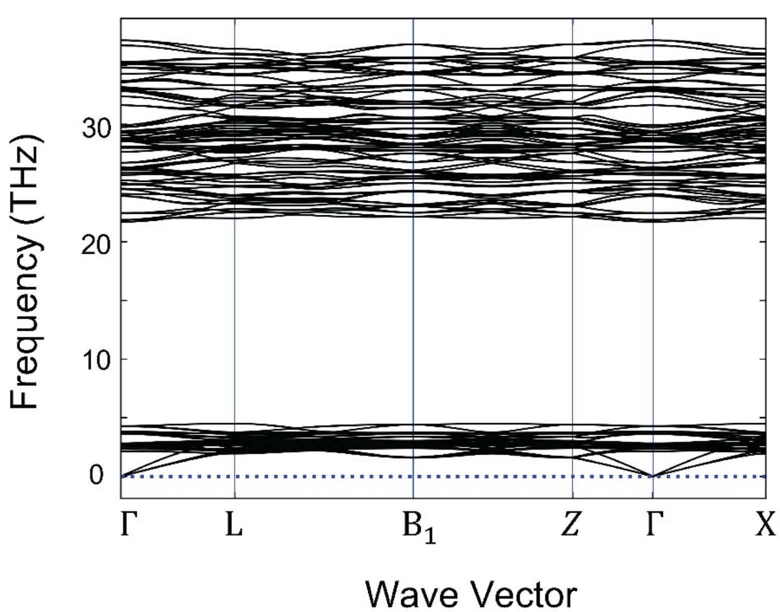
30
20
10
0
Frequency (THz)
Γ
L
B1
Z
Γ
X
Wave Vector

Supplementary Figure S5. Comparison of the electronic density of states (DOSs) between R3C and Pm-3n structure of $\beta - UH_3$ calculated by PBE+U(0.6).

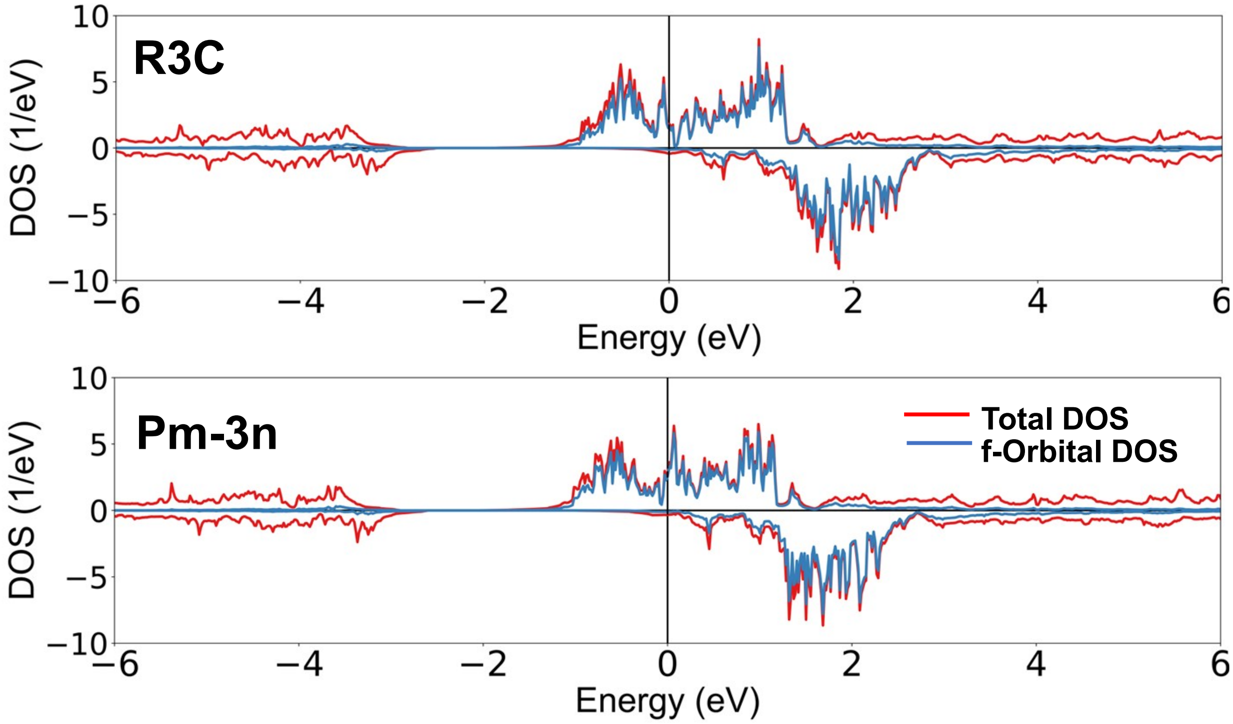

Supplementary Table S2. Pm-3n and R3C structures that were optimized by PBE+U(0.6) in VASP POSCAR format.

$\beta - UH_3$ PBE+U(0.6)	Optimized Structure (VASP POSCAR)
Pm-3n	b-UH3 (Pm-3n, PBE+U(0.6)) 1 6.618726373 0.000000000 0.000000000 0.000000000 6.618726373 0.000000000 0.000000000 0.000000000 6.618726373 U H 8 24 Direct 0.000000 0.000000 0.000000 0.250000 0.000000 0.500000 0.000000 0.500000 0.750000 0.000000 0.500000 0.250000 0.500000 0.250000 0.000000 0.750000 0.000000 0.500000 0.500000 0.750000 0.000000 0.500000 0.500000 0.500000 0.000000 0.155154 0.304729 0.195271 0.344846 0.500000 0.804729 0.344846 0.500000 0.500000 0.195271 0.344846 0.500000 0.804729 0.655154 0.344846 0.500000 0.195271 0.655154 0.500000 0.195271 0.155154 0.695271 0.000000 0.695271 0.000000 0.844846 0.695271 0.000000 0.155154 0.844846 0.304729 0.000000 0.304729 0.000000 0.844846 0.844846 0.695271 0.000000 0.155154 0.304729 0.000000 0.304729 0.000000 0.155154 0.195271 0.655154 0.500000 0.000000 0.155154 0.695271 0.804729 0.655154 0.500000 0.500000 0.804729 0.344846 0.000000 0.844846 0.695271 0.500000 0.195271 0.655154 0.655154 0.500000 0.804729 0.000000 0.844846 0.304729 0.344846 0.500000 0.804729

R3C	b-UH3 (R3C, PBE+U(0.6)) 1 6.628754273 0.013973369 -0.013973564 0.013973564 6.628754273 -0.013973369 -0.013973369 -0.013973564 6.628754273 U H 8 24 Direct 0.002554 0.002554 0.997446 0.253265 0.004679 0.499974 0.004679 0.500026 0.746735 0.000026 0.504679 0.246735 0.500026 0.253265 0.995321 0.753265 0.000026 0.495321 0.504679 0.753265 0.999974 0.502554 0.502554 0.497446 0.002229 0.157575 0.302130 0.198130 0.347798 0.495883 0.807168 0.346664 0.495760 0.502229 0.197870 0.342425 0.504240 0.807168 0.653336 0.346664 0.504240 0.192832 0.656576 0.502308 0.192584 0.157575 0.697870 0.997771 0.697870 0.002229 0.842425 0.698130 0.004117 0.152202 0.846664 0.307168 0.995760 0.307416 0.002308 0.843424 0.847798 0.698130 0.995883 0.156576 0.307416 0.997692 0.307168 0.004240 0.153336 0.197870 0.657575 0.497771 0.002308 0.156576 0.692584 0.807416 0.656576 0.497692 0.502308 0.807416 0.343424 0.004240 0.846664 0.692832 0.504117 0.198130 0.652202 0.657575 0.502229 0.802130 0.004117 0.847798 0.301870 0.347798 0.504117 0.801870

Supplementary Figure S6. Comparison of the simulated XRD patterns for Pm-3n and distorted R3C for $\beta - UH_3$.

In the main body, we suggest two possible explanations for the structural change of $\beta - UH_3$ from Pm-3n to R3C, which was caused by the use of $U_{eff} = 0.6\ eV$ for PBE. The second one is that R3C may in fact be the ground state, but due to the difficulty in distinguishing the difference in the X-ray diffraction (XRD) patterns of the Pm-3n and R3C structures, especially at finite temperatures, it has not been classified correctly by experiments. Figure (a) and the broken lines in (b) use 0.2 degrees as the FWHM, which is comparable with experimental data,[3] while the solid lines in (b) use 0.01 degrees to show the peak splitting. Each peak intensity is normalized so that the maximum peak height is 1. The location and intensity of the XRD peaks show no clear differences between the two structures, not only for these three peaks but also for all major peaks. If a small FWHM is applied, it can be observed that the R3C structure has double peaks, whereas the Pm-3n structure has a single peak, as shown in Figure (b). However, with the same FWHM as the experimental value, it is difficult to distinguish the double peaks of the R3C structure, and thus, there exists the possibility of a distorted ground state.

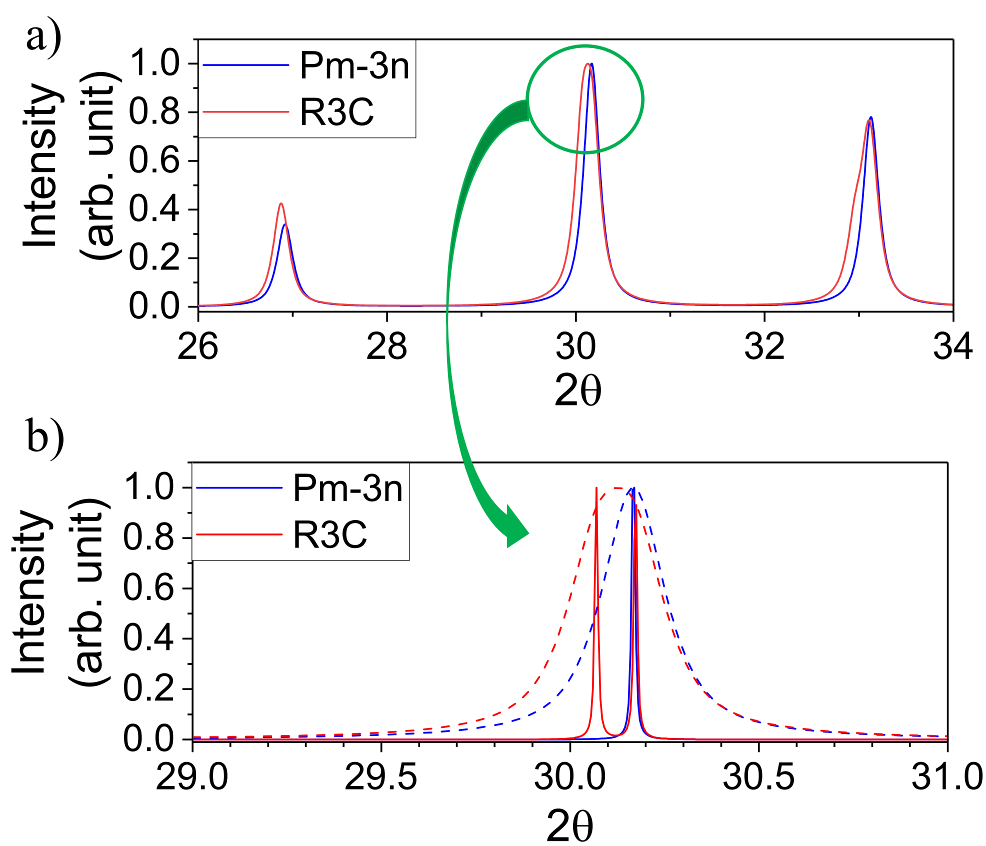

Supplementary Table S3. The formation energies and lattice constants of the FM, SQS, AFM and NM models with PBE+U(0.6) used to generate Figure 9 of the main body.

		FM	SQS	AFM	NM
Formation Energy (eV)	$\alpha - UH_3$	-1.337	-1.250	-1.156	-0.830
	$\beta - UH_3$	-1.368	-1.306	-1.260	-0.848
Lattice Constant (Å)	$\alpha - UH_3$	4.134	4.128	4.118	4.042
	$\beta - UH_3$	6.619	6.619	6.613	6.470

Supplementary Table S4. Calculation results of hydrostatic pressure – volumetric strain relation used to generate Figure 11 of the main body.

Volumetric Strain	Hydrostatic Stress (GPa)			
	FM PBE	FM PBE+U(0.6)	AFM PBE+U(0.6)	SQS PBE+U(0.6)
-0.271	58.96	57.52	56.79	57.90
-0.246	49.08	47.90	47.14	47.63
-0.221	40.19	39.32	38.55	39.82
-0.196	32.24	31.67	30.96	31.20
-0.169	25.19	25.13	24.28	25.74
-0.143	18.98	20.28	18.40	19.86
-0.115	13.78	15.79	13.25	14.76
-0.087	10.02	11.27	10.52	10.29
-0.059	6.88	7.10	6.59	6.37
-0.030	3.35	3.33	3.09	2.97
0.0	0.00	0.00	0.00	0.00
0.030	-2.98	-2.87	-2.48	-2.53
0.061	-5.57	-5.33	-4.49	-4.74
0.093	-7.81	-7.46	-6.15	-6.73

Reference

1. Fontaine DD. Cluster Approach to Order-Disorder Transformations in Alloys. In: Solid State Physics [Internet]. Elsevier; 1994 [cited 2019 Mar 22]. p. 33–176. Available from: https://linkinghub.elsevier.com/retrieve/pii/S0081194708606396

2. Van De Walle A, Tiwary P, De Jong M, Olmsted DL, Asta M, Dick A, et al. Efficient stochastic generation of special quasirandom structures. Calphad Comput Coupling Phase Diagr Thermochem. 2013;42:13–18.

3. Ao B, Wang X, Wei Y, Zhang Y. A simple hermetic sample holder for X-ray diffraction analysis of uranium hydride. J Appl Crystallogr. 2007 Aug 1;40(4):796–8.

4. Miranda H. Phonons [Internet]. 2019 [cited 2019 Jul 5]. Available from: http://henriquemiranda.github.io/